European Spine Journal (2019) 28:2169–2178
https://doi.org/10.1007/s00586-019-06007-z

ORIGINAL ARTICLE

A comparative study of diffusion kurtosis imaging and T2* mapping in quantitative detection of lumbar intervertebral disk degeneration

Feifei Zeng[1] · Yunfei Zha[1] · Liang Li[1] · Dong Xing[1] · Wei Gong[1] · Lei Hu[1] · Yang Fan[2]

Received: 2 October 2018 / Revised: 6 March 2019 / Accepted: 9 May 2019 / Published online: 15 May 2019

Abstract

Purpose To assess the feasibility of diffusion kurtosis imaging (DKI) for diagnosing lumbar intervertebral disk degeneration (IDD) and to compare the potential of DKI and T2* mapping in the diagnosis of early IDD.

Methods Sagittal T2WI, DKI, and T2* mapping were performed in 75 subjects with 375 lumbar intervertebral disks at a 3.0-T MRI. DKI-related parameters including mean kurtosis (MK), mean diffusivity (MD), fractional anisotropy (FA), and T2* values were calculated for each disk which was segmented into three regions: nucleus pulposus (NP), anterior annulus fibrosus (AAF), and posterior annulus fibrosus (PAF).

Results MK and FA were positively correlated with Pfirrmann grade (all $P<0.001$). MD and T2* were negatively correlated with Pfirrmann grade (all $P<0.001$) except for T2* value of AAF ($r=0.087$, $P>0.05$). MK and FA values increased, while MD and T2* values decreased with age. No statistical significance was found between men and women ($P>0.05$). Cephalic lumbar disks (L1/L2 and L2/L3) got lower MK and FA values than caudal lumbar disks (L4/L5 and L5/S1) (all $P<0.05$), while cephalic lumbar disks got higher MD value than caudal lumbar disks (all $P<0.05$). ROC analysis demonstrated that MK, MD, and FA showed significantly higher diagnostic accuracies than T2*, especially in NP and PAF.

Conclusions DKI can be used to assess human lumbar IDD. And DKI was more sensitive to the quantitative detection of early lumbar IDD than T2* mapping.

Graphical abstract

These slides can be retrieved under Electronic Supplementary Material.

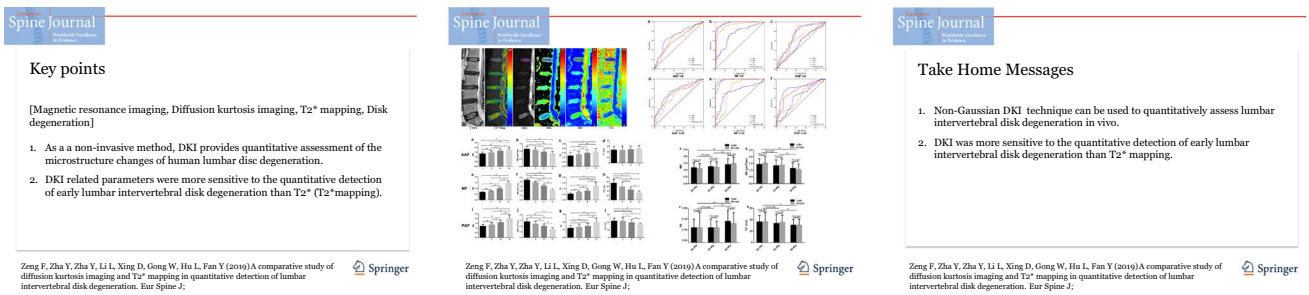

Keywords Magnetic resonance imaging · Diffusion kurtosis imaging · T2* mapping · Disk degeneration

Introduction

Low back pain (LBP) is a universal, social, and economic health problem worldwide. Lumbar spine-related LBP is caused predominantly by intervertebral disk degeneration (IDD) [1]. The intervertebral disk (IVD), a fibrocartilaginous joint, is composed of the nucleus pulposus (NP), annulus

Electronic supplementary material The online version of this article (https://doi.org/10.1007/s00586-019-06007-z) contains supplementary material, which is available to authorized users.

✉ Yunfei Zha
yunfei_zha2018@163.com

Extended author information available on the last page of the article

fibrosus (AF), and cartilaginous endplate. Multiple factors, such as cell aging, dystrophia, biomechanical changes, and biomechanical factors, lead to proteoglycan (PG) degradation and loss of collagen and water content, resulting in IDD [2]. It is crucial to identify early biochemical markers of IDD that would be helpful in improving therapy strategies and prognoses at its early stage.

The change in the molecular diffusion of water is also regarded as a marker of early lumbar IDD [3]. Additionally, the lumbar IVD is the most massive avascular tissue in the adult human body, and its main supply of nutrient is reliant on metabolic pathways from vertebral endplate. These extraordinary anatomical and physiological properties make it harder to self-repair in comparison with other organs. Also, IDD is believed to begin as early as in the second decade of life [4]. It is, therefore, essential to identify early biochemical markers that are conducive to the precaution of degenerative disk disease at its early phase. The identification of these markers would require the use of experimental techniques.

T2* mapping, a technique with distinct features including speed of imaging, high image resolution, and isotropic three-dimensional (3D) cartilage evaluation, is sensitive to collagen fiber network. Recent studies have demonstrated a close correlation between T2* mapping and Pfirrmann grade, where a decrease in T2* value is significantly associated with the aggravation of IDD [5, 6]. Pathologically, T2* value is regarded as a robust biomarker at an earlier stage of IDD [7].

Diffusion magnetic resonance imaging techniques, such as diffusion-weighted imaging (DWI) and diffusion tensor imaging (DTI), are noninvasive and quantitative techniques that can assess IDD by offering information about the properties of the water molecular diffusion process in IVD [8]. These models assume a free and unrestricted behavior of water diffusion. However, in vivo tissues, the diffusion of water molecules has been shown to be hindered and restricted by complex microstructures, leading to a non-Gaussian probability distribution function (PDF) [9]. The illustration of MR signal loss curve as a function of b value for Gaussian (DTI) and non-Gaussian (DKI) models of water diffusion is shown in Fig. 1 [10]. Diffusion kurtosis imaging (DKI) as a non-Gaussian model has a higher potential to characterize both molecular water diffusion and the complexity of tissue microstructures. DKI technique can provide several quantitative parameters, such as the mean, axial, and radial kurtosis (MK, $K\parallel$, $K_{\perp}$), the mean, axial, and radial diffusivities (MD, $D\parallel$, $D_{\perp}$), and fractional anisotropy (FA). MK is defined as the kurtosis averaged among all directions. MD corresponds to the average of the diffusion coefficient over all directions. FA describes the fraction of the tensor that can be assigned to anisotropic diffusion [11]. A DKI study of the IVD in matured SD rats demonstrated that MK and fractional FA produced higher diagnostic accuracies for early IDD, compared to apparent diffusion coefficient (ADC) [12]. In previous studies, the DKI technique has demonstrated a remarkable success in characterizing the grade of neural tumors, prostate cancer, breast cancer, identification of pulmonary nodule and sinonasal lesions, and other diseases [13–17]. However, the application of DKI on human IDD has not been reported before.

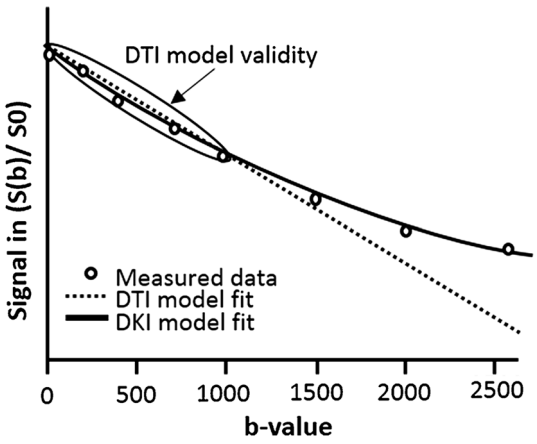

Fig. 1 Illustration of MR signal loss curve as a function of *b* value for Gaussian (DTI) and non-Gaussian (DKI) models of water diffusion [10]

This preliminary study aimed to use a quantitative new DKI approach to assess human lumbar IDD and to compare the potential of DKI and T2* mapping in the diagnosis of early IDD.

Materials and methods

Study subjects

This prospective study was approved by the local institutional review board, and written informed consent was obtained from all subjects. Patients suffering from single or recurrent episodes LBP or sciatica in the last 6 months were included. The exclusion criteria were as follows: previous spinal surgery, chemoradiotherapy, spinal tumor, spinal tuberculosis, serious scoliosis, and other previously diagnosed abnormalities of the lumbar spine. Subjects were divided into three age groups: group 20–34 y, group 35–49 y, and group 50–65 y.

MR imaging technique

All the participants underwent the MR scan including sagittal T2-weighted imaging (T2WI), T2* mapping, and DKI imaging on a 3.0-T MR scanner (Discovery MR750, GE

Healthcare) with a spine-array coil covering the IVDs L1/L2 to L5/S1. T2-weighted images were scanned using a fast spin echo sequence (FSE) with the following parameters: a repetition time (TR)/echo time (TE) = 2500 ms/120 ms, slice thickness/gap = 4 mm/0.5 mm, field of view (FOV) = 30 cm × 30 cm, and matrix = 352 × 320. For acquisition of DKI, a single-shot echo-planar imaging sequence (SS-EPI) was performed with three b values of 0, 1000, and 2000 s/mm^2 and 30 diffusion directions for every nonzero b value, TR = 2000 ms, TE = 71.7 ms, slice thickness/gap = 4 mm/0.5 mm, FOV = 30 cm × 15 cm, and in-plane matrix = 128 × 128. T2* mapping was obtained using a multi-echo gradient echo (GRE) sequence with the following parameters: TR = 73.3 ms, TE = 1.6, 3.9, 6.2, 8.5, 10.8, 13.1, 15.4, and 17.7 ms, slice thickness/gap = 4 mm/0.5 mm, FOV = 30 cm × 30 cm, and matrix = 256 × 256.

Image analysis

Two radiologists with more than 10 years of experience in MR imaging of the spine graded all lumbar IVDs on the T2-weighted images according to the Pfirrmann grade system (Table 1) [18].

The acquired MR images (grades I–IV) were transferred to a vendor-offered workstation (Advantage Workstation 4.6, GE Healthcare) for post-processing. In Function tool software, T2* maps for each subject were obtained using a mean square linear fit algorithm on multi-echo GRE images by R2 star. In addition, the DKI-related parameters, such as MK, MD, and FA, were fitted using the kurtosis model [10].

Regions of interest (ROIs) were manually drawn on the midline slice of sagittal DKI (b0 images) and T2* maps at five equally sized circular ROIs from anterior (ROI 1) to posterior (ROI 5) to obtain information on spatial variation between the anterior annulus fibrosus (ROI 1), the nucleus pulposus (ROI 2–ROI 4), and posterior annulus fibrosus (ROI 5). The mean value of ROI 1–ROI 5 was treated as the averaged measurements of a whole disk. Then, these ROIs were generated to the calculated parametric maps. For each disk, DKI-derived parameters (MK, MD, and FA) and T2* values were measured. The placement of different ROIs for a typical subject on each parametric map is illustrated in Fig. 2.

Statistical analysis

All statistical analyses were performed with SPSS software (version 20.0, SPSS, Chicago, Ill). The mean value of each parameter (MK, MD, FA, and T2*) for each subject was used for quantitative statistical analyses.

All values of each subject were analyzed using ANOVA and Dunnett's T3 test for the comparison of all four grades (grades I–IV). Spearman correlation was performed to investigate the relationship between values of each computed parameter and Pfirrmann grade. Pearson correlation was performed to investigate the relationship between values of each computed parameter and age, and Dunnett's T3 test was used for the pairwise comparison of age groups. Mann–Whitney *U* test was used to examine statistical differences of parameters between genders. And Dunnett's T3 test was used to examine statistical differences of parameters (MK, MD, FA, and T2*) between cephalic disks (L1/L2 and L2/L3) and caudal lumbar disks (L4/L5 and L5/S1). Receiver operating characteristic curves (ROC) were generated for each parameter to assess the area under the receiver operating characteristic curve (AUC), sensitivity and specificity for differentiating Pfirrmann grade I from grade II disks, and grade II from grade III disks. A *P* value less than 0.05 was considered as statistically significant.

Results

Pfirrmann grade distribution

Seventy-five subjects (mean age 39.6 ± 14.6 years; range 20–65 years) including 36 males (mean age 38.8 ± 14.7 years; range 20–63 years) and 39 females (mean age 40.2 ± 14.5 years; range 22–65 years) were recruited in this study. A total of 369 intervertebral lumbar disks from L1/L2 to L5/S1 were scanned. Table 2 shows the number

Table 1 Pfirrmann grades of disk degeneration [18]

Grade	Structure	Distinction of nucleus and annulus	Signal intensity	Height of intervertebral disk
I	Homogeneous, bright white	Clear	Hyperintense, isointense to cerebrospinal fluid	Normal
II	Inhomogeneous with or without horizontal bands	Clear	Hyperintense, isointense to cerebrospinal fluid	Normal
III	Inhomogeneous, gray	Unclear	Intermediate	Normal to slightly decreased
IV	Inhomogeneous, gray to black	Lost	Intermediate to hypointense	Normal to moderately decreased
V	Inhomogeneous, black	Lost	Hypointense	Collapsed disk space

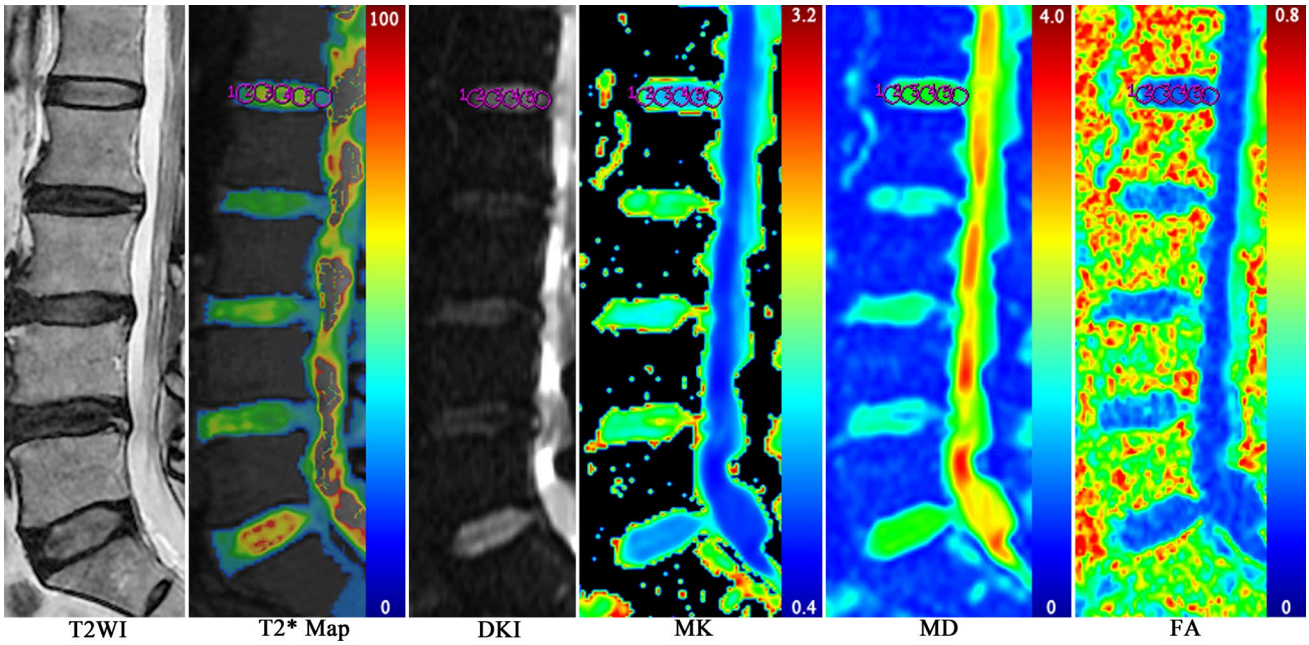

Fig. 2 MR images of the lumbar spine in a 55-year-old woman. Every lumbar IVD was cut into 5 uniform parts in each DKI (b0), MK, MD, FA, and T2* map, and ROI 1 represented AAF, ROI 5 represented PAF, the average value of ROI 2, ROI 3, and ROI 4 represented NP. Based on the Pfirrmann grade, L1/L2 and L5/S1 were graded as Pfirrmann grade II, L2/L3 and L4/L5 were graded as Pfirrmann grade IV, and L3/L4 was graded as Pfirrmann grade III

Table 2 Number of IVDs in various age groups of male and female according to Pfirrmann grades

Gender	Age groups	Number of person	Number of intervertebral disks			
			I	II	III	IV
Male	Group 20–34 y	19	44	45	6	0
	Group 35–49 y	8	8	18	10	4
	Group 50–65 y	9	2	12	20	9
Female	Group 20–34 y	20	45	47	8	0
	Group 35–49 y	8	10	14	11	5
	Group 50–65 y	11	5	4	25	17

of IVDs and the Pfirrmann grade distribution of male and female in each age group.

Between-grades differences in different disk segments

According to Pfirrmann grade, significant difference was found in all parameters for all segments except T2* value of AAF ($P > 0.05$) (Table 3). MK and FA values increased and MD and T2* values decreased with Pfirrmann grades. Post hoc multiple comparisons showed statistical significance in most degeneration groups (Fig. 3). The robust difference was observed in NP for MK, MD, and FA comparisons (all $P < 0.001$). For T2* value, it showed less difference among degeneration groups, especially in AAF and PAF. For different segments of IVD, a statistically significant difference was found in all metrics (all $P < 0.05$), except the FA value between AAF and PAF ($P > 0.05$).

Spearman correlation analysis

Pfirrmann grades were significantly correlated with all measured parameters in AAF, NP, and PAF (Table 4). MK and FA values were positively correlated with Pfirrmann grade (all $P < 0.001$), while MD and T2* values were negatively correlated with Pfirrmann grade (all $P < 0.001$) except for T2* value of AAF ($r = 0.098$, $P > 0.05$). Comparing the Spearman correlation coefficient, the highest correlation value was seen in NP and lowest r value was seen in AAF. In addition, the DKI-derived MK and MD had higher correlation values

Table 3 DKI parameters and T2* value of NP, AAF, and PAF with Pfirrmann grades

Number		Pfirrmann grade				*F* value	*P* value
		I	II	III	IV		
		114	140	80	35		
AAF	MK	1.37 ± 0.20	1.46 ± 0.22	1.63 ± 0.23	1.81 ± 0.27	65.065	< 0.001
	MD	1.17 ± 0.19	1.10 ± 0.19	0.96 ± 0.15	0.85 ± 0.16	39.651	< 0.001
	FA	0.12 ± 0.04	0.14 ± 0.04	0.15 ± 0.04	0.16 ± 0.04	20.658	< 0.001
	T2*	23.53 ± 6.94	22.73 ± 8.53	24.63 ± 7.15	25.72 ± 7.21	1.349	0.251
NP	MK	0.67 ± 0.04	0.78 ± 0.04	0.99 ± 0.14	1.44 ± 0.19	739.247	< 0.001
	MD	2.21 ± 0.10	1.95 ± 0.10	1.56 ± 0.18	1.07 ± 0.13	822.923	< 0.001
	FA	0.05 ± 0.01	0.07 ± 0.01	0.08 ± 0.02	0.12 ± 0.04	222.749	< 0.001
	T2*	74.67 ± 17.45	59.06 ± 19.07	45.65 ± 10.99	32.68 ± 7.13	69.179	< 0.001
PAF	MK	1.20 ± 0.20	1.36 ± 0.21	1.60 ± 0.21	2.01 ± 0.37	125.381	< 0.001
	MD	1.41 ± 0.19	1.21 ± 0.21	1.01 ± 0.18	0.72 ± 0.16	97.907	< 0.001
	FA	0.12 ± 0.03	0.14 ± 0.04	0.15 ± 0.04	0.20 ± 0.05	29.935	< 0.001
	T2*	21.71 ± 3.60	21.57 ± 4.70	19.71 ± 3.50	17.11 ± 1.70	12.740	< 0.001

Values represent mean ± SD. Units for MK and FA values are dimensionless. MD value is given in $\mu m^2/ms$. T2* value is given in ms

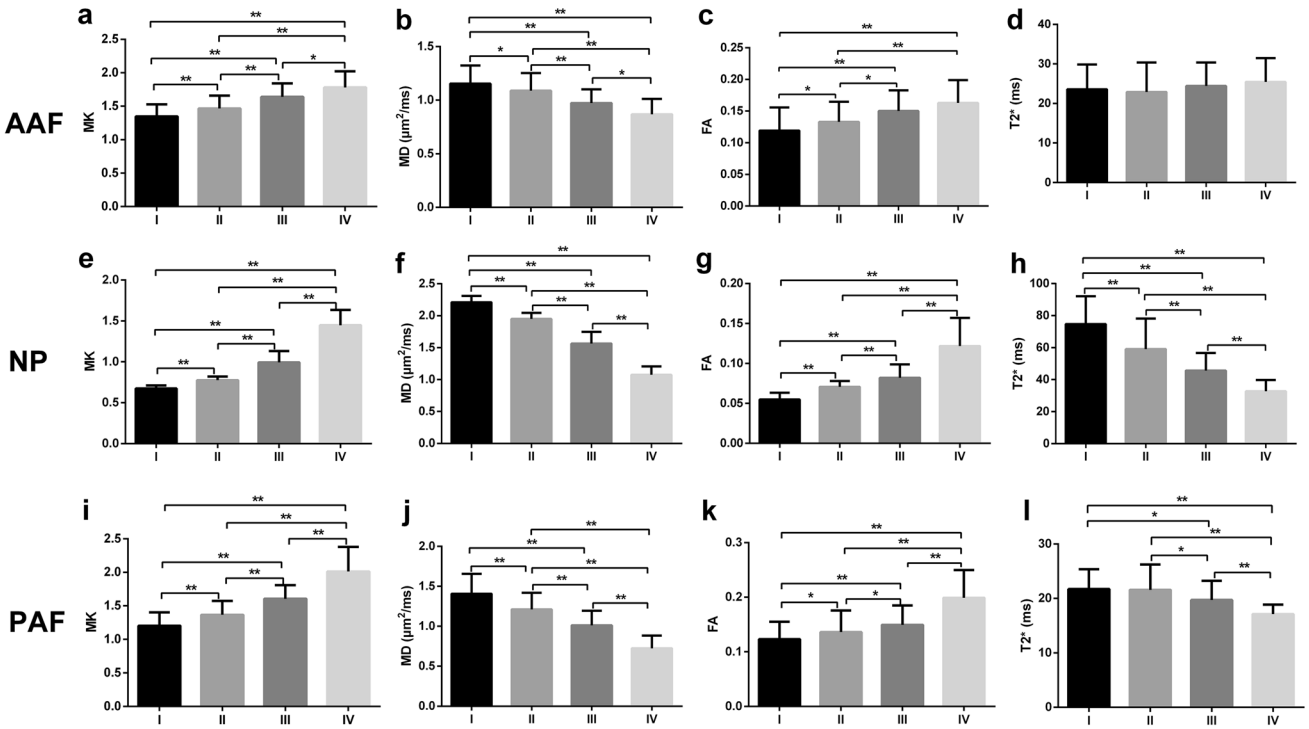

Fig. 3 Post hoc multiple comparisons among four Pfirrmann grades. MK and FA values increased and MD and T2* values decreased with Pfirrmann grades. No statistical significance was found in the comparisons of grades III and IV of AAF's FA value, grade I and grade II of PAF's T2* value, and all grades of AAF's T2* value (all $P > 0.05$). And the other multiple comparisons showed significant differences (all $P < 0.05$). *P values of 0.05 and **P values of < 0.001 were considered statistically significant by multiple comparisons

with Pfirrmann grades than FA and T2*. Furthermore, no matter in nucleus pulposus or in annulus fibrosus, DKI parameters held higher *r* values than T2* value.

Evaluation of disk's MK, MD, FA, and T2* values with age and sex

The Pearson correlation coefficient between computed parameters (MK, MD, FA, and T2*) of the whole disk and

Table 4 Spearman correlation analysis of MK, MD, FA, and T2* values with Pfirrmann grade

Spearman correlation analysis	AAF				NP				PAF			
	MK	MD	FA	T2*	MK	MD	FA	T2*	MK	MD	FA	T2*
r value	0.587	−0.500	0.433	0.098	0.934	−0.929	0.792	−0.670	0.685	−0.663	0.408	−0.336
P value	<0.001	<0.001	<0.001	0.059	<0.001	<0.001	<0.001	<0.001	<0.001	<0.001	<0.001	<0.001

age was 0.560, −0.625, 0.497, and −0.403, respectively (all $P<0.001$). The average values of the whole disk in each age group are shown in Fig. 4. MK and FA values increased and MD and T2* values decreased with age. Furthermore, a significant difference was found between group 50–65 y and other two groups (group 20–34 y and group 35–49 y) ($P<0.05$) in all computed parameters (MK, MD, FA, and T2*), while no significant difference was found between group 20–34 y and group 35–49 y ($P>0.05$). A Mann–Whitney *U* test demonstrated no statistical significance between men and women for all computed parameters (MK, MD, FA, and T2*) in all age groups ($P>0.05$).

Evaluation of disk's MK, MD, FA, and T2* values with spinal levels

The Dunnett's T3 test result of parameters between cephalic disks (L1/L2; L2/L3) and caudal lumbar disks (L4/L5; L5/S1) is depicted in Fig. 5. Statistically significant metrics were observed between upper disks and lower lumbar disks. Disks at L1/L2 (1.16 ± 0.18) got lower MK value than disks at L4/L5 (1.30 ± 0.23, $P<0.05$), and disks at L1/L2 and L2/L3 (1.20 ± 0.20) got lower MK value than disks at L5/S1 (1.43 ± 0.33, all $P<0.001$), while disks at L1/L2 (1.46 ± 0.19 μm^2/ms) got higher MD value than disks at L4/L5 (1.34 ± 0.25 μm^2/ms, $P<0.05$), and disks at L1/L2 and L2/L3 (1.43 ± 0.22 μm^2/ms) got higher MD value than disks at L5/S1 (1.21 ± 0.28 μm^2/ms, all $P<0.001$). Disks at L1/L2 (0.11 ± 0.02) and L2/L3 (0.11 ± 0.02) got lower FA value than disks at L5/S1 (0.14 ± 0.03, all $P<0.001$).

Diagnostic value comparison

Table 5 and Fig. 6 demonstrate the diagnostic performance of all metrics. All AUC values ($P<0.05$) had notable significance except the AUC values of T2* of AAF and PAF

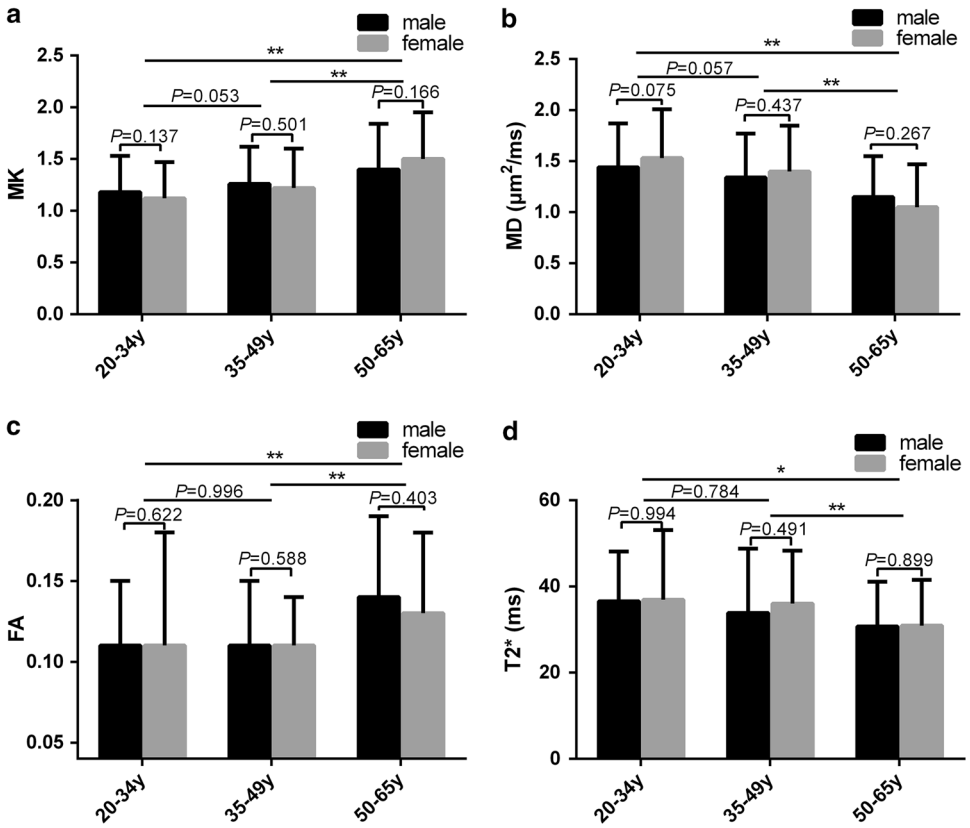

Fig. 4 Intervertebral disk's DKI parameters and T2* value in different genders and age groups. The comparison of MK (**a**), MD (**b**), FA (**c**), and T2* (**d**) values in male and female (the shorter line) among group 20–34 y, group 35–49 y, and group 50–65 y (the upper and longer line) was made. Significant difference was found between group 50–65 y and the other two groups (group 20–34 y and group 35–49 y) in all computed parameters, while no significant difference was found between men and women for all computed parameters (MK, MD, FA, and T2*) in all age groups. *P values of <0.05 and **P values of <0.001 were considered statistically significant by multiple comparisons

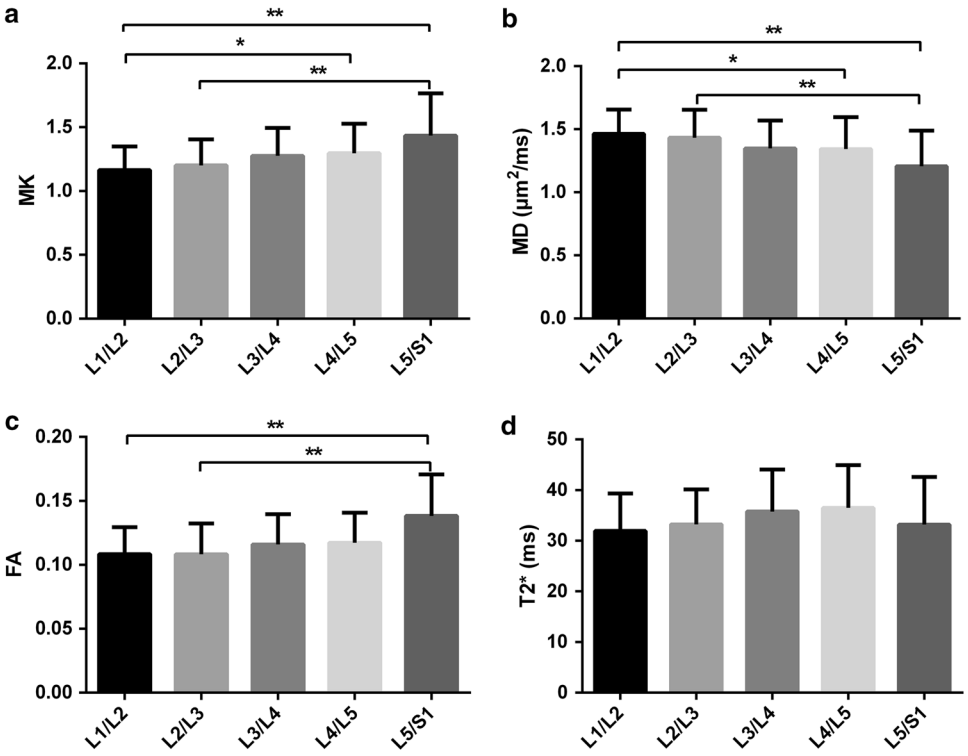

Fig. 5 The comparison of MK (**a**), MD (**b**), FA (**c**), and T2* (**d**) values at different spinal levels. Statistically significant MK, MD, and FA values were observed between upper disks and lower lumbar disks. *P values of <0.05 and **P values of <0.001 were considered statistically significant by multiple comparisons

Table 5 ROC analysis of MK, MD, FA, and T2* for differentiating grade I from grade II disks and grade II from III disks

ROC analysis		Pfirrmann grades I–II				Pfirrmann grades II–III			
		AUC (95% CI)	Sensitivity (%)	Specificity (%)	Cutoff	AUC (95% CI)	Sensitivity (%)	Specificity (%)	Cutoff
AAF	MK	0.694 (0.628–0.760)	63.6	74.6	1.44	0.744 (0.678–0.811)	72.9	68.7	1.56
	MD	0.625 (0.556–0.693)	52.1	68.4	1.08	0.707 (0.638–0.776)	66.4	70.0	1.04
	FA	0.646 (0.577–0.715)	67.9	63.2	0.12	0.665 (0.590–0.740)	78.6	51.2	0.15
NP	MK	0.976 (0.962–0.990)	85.7	97.4	0.73	0.988 (0.978–0.997)	93.6	95.0	0.84
	MD	0.973 (0.956–0.991)	86.4	96.5	2.05	0.975 (0.958–0.992)	94.3	88.7	1.80
	FA	0.918 (0.880–0.955)	76.4	94.7	0.06	0.772 (0.696–0.848)	90.7	66.2	0.08
	T2*	0.738 (0.677–0.800)	75.0	69.3	65.88	0.737 (0.670–0.805)	61.7	82.5	52.11
PAF	MK	0.734 (0.658–0.787)	80.7	61.4	1.22	0.806 (0.746–0.866)	80.0	78.7	1.51
	MD	0.722 (0.664–0.793)	90.7	57.0	1.38	0.760 (0.695–0.825)	59.3	86.3	1.16
	FA	0.607 (0.536–0.677)	55.0	69.3	0.12	0.613 (0.537–0.690)	78.6	43.7	0.15
	T2*	0.543 (0.472–0.615)[#]	69.7	49.1	21.68	0.620 (0.542–0.699)	62.1	62.2	20.2

[#]P values of >0.05 were considered without statistical significance. Units for MK and FA values are dimensionless. MD value is given in μm^2/ms. T2* value is given in ms

($P>0.05$) for differentiating Pfirrmann grade I from grade II disks. The AUC values of the metrics for differentiating Pfirrmann grade I from grade II disks, and grade II from III disks, ranked as follows: MK > MD > FA > T2*. As the AUC values were greater than 0.500, DKI parameters could be considered as significant predictors for early IDD. What is more, DKI parameters had mostly greater sensitivity and specificity. For different parts, the rank of the diagnostic accuracy was NP > PAF > AAF. Additionally, in NP segment, the AUC values of MK and MD for differentiating Pfirrmann grade I from grade II disks, and grade II from III disks as well as FA for differentiating Pfirrmann grade I from grade II disks, were larger than 0.900, which showed that MK, MD, and FA could serve as great significant predictors for early NP degeneration. Overall, for early lumbar IDD, DKI parameters showed significantly higher diagnostic accuracy than T2* in all segments, especially in NP and PAF.

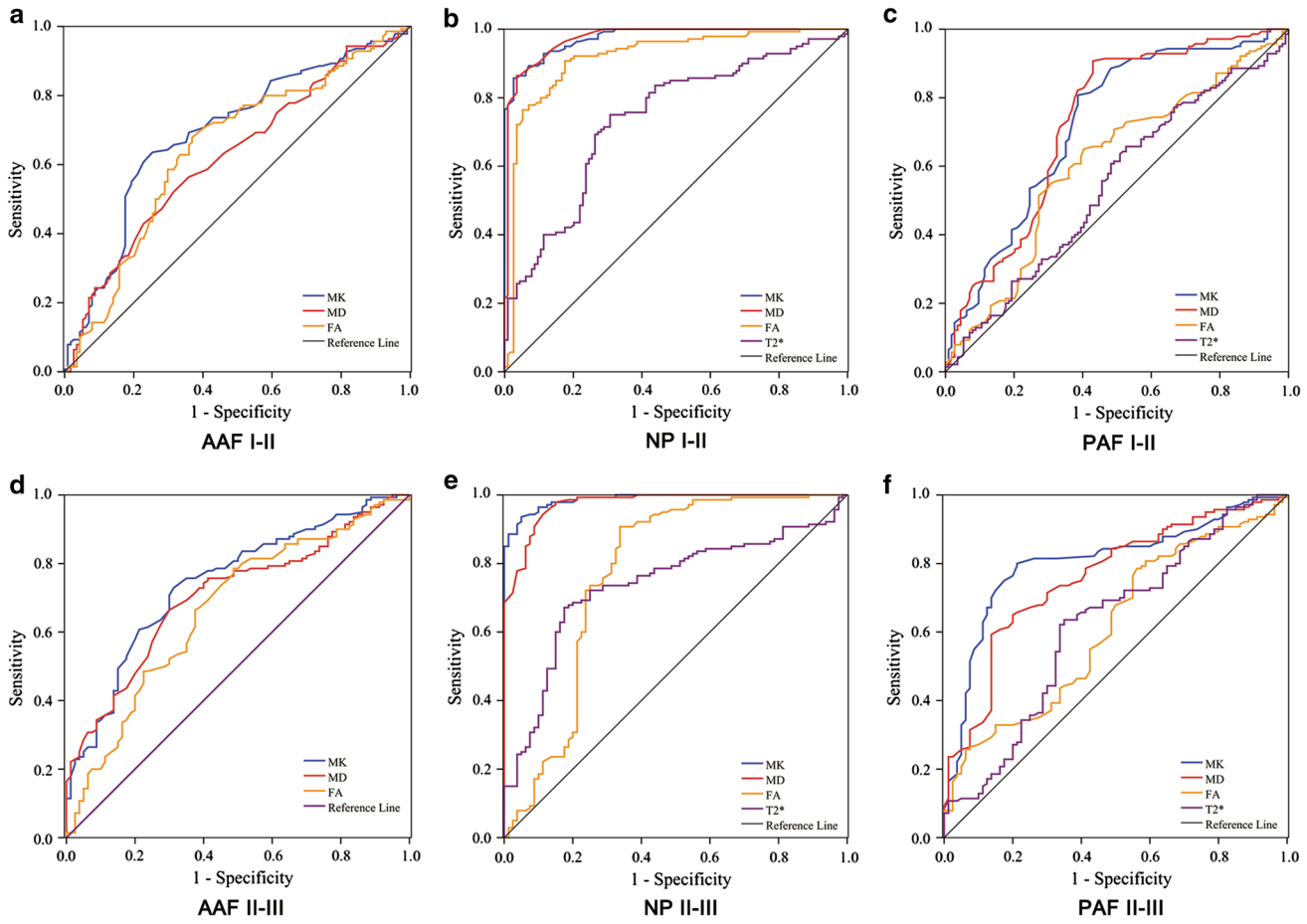

Fig. 6 ROC analysis. Plots **a** (AAF), **b** (NP), and **c** (PAF) demonstrate the results of the ROC analysis for differentiating Pfirrmann grade I from grade II disks. Plots **d** (AAF), **e** (NP), and **f** (PAF) demonstrate the results of the ROC analysis for differentiating Pfirrmann grade II from III disks. DKI parameters (MK, MD, and FA) got higher AUC values than T2* in all segments, especially in NP and PAF

Discussion

Our results revealed that both DKI and T2* mapping techniques played essential roles in the quantitative assessment of lumbar IDD. MK and FA values correlated positively with Pfirrmann grades, while MD and T2*values correlated negatively with Pfirrmann grades, except for the AAF's T2* value. MK and FA values increased, while MD and T2* values decreased with age. No statistical significance was found between men and women for all computed parameters (MK, MD, FA, and T2*) in all age groups. Significant differences in metrics (MK, MD, and FA) were observed between upper disks and lower lumbar disks. ROC analyses demonstrated that DKI parameters (MK, MD, and FA) conveyed significantly higher diagnostic accuracies in identifying Pfirrmann grade I from grade II disks, and grade II from grade III disks, especially in NP and PAF, compared to T2* values.

Non-Gaussian DKI provides a higher-order description of a restricted water diffusion process by a second-order three-dimensional (3D) diffusivity tensor together with a fourth-order 3D kurtosis tensor, which reportedly offers an improved sensitivity in detecting developmental and pathological changes in tissues, compared to conventional DWI and DTI [9, 19]. A previous study carried out on rats established that decreased ADC and increased FA and MK values were observed in grade II when compared to grade I results [12]. Our results are consistent with those findings quantitatively. That MK and FA values correlated positively with Pfirrmann grade, while MD values displayed a negative correlation in this study, suggests that the degenerative process was in play. As the quantity and quality of PG diminish, the collagen fibrils in the disk become sprawling with disk degeneration, which could be one of the underlying reasons for the increased MK values. Fewer PGs and weaker osmotic pressures result in the loss of water and an increase in collagen fibrils [20]. These changes restrict water diffusion within the disk, which may explain the decrease in MD potentially. The increase in FA

could mean anatomical changes in degenerated disks are triggered. The fibers of a standard AF rank in a concentric circle regularly [21]. However, with degeneration, granulation tissues, nerves, and vascellum expand from the outer AF region into the inner region, and the inner AF region expands into an NP region, which alters the disk's normal anatomy from order to disorder [20]. Thus, an increase in FA value may arise from various directions.

IDD is believed to be an inevitable consequence of aging. Several enzymes degrade the matrix, destroy hydrophilic glycosaminoglycans (GAGs) within the NP, and lead to the accumulation of cleaved extracellular matrix fragments with disk aging [22]. NP cells are involved in repairing and replacing the diminishing extracellular matrix during age-related degeneration [23]. The result of our current study showed that MK and FA values increased and MD and T2* values decreased with age. Additionally, MK, MD, and FA values obtained by DKI highly correlated with age than by T2* value. Interestingly, the disks' parameters of the 50–65 years age group had statistically significant differences when compared to the 20–34 and 35–49 years age groups, while no significant difference was found between the 20–34 and 35–49 years age groups. Such results would suggest that most of the disks changed from Pfirrmann grade I to III, stabilized in 20–50 years old, and underwent a rapid degenerative process after 50 years old, in line with an earlier report [24].

In our investigation, no statistical significance was found between men and women for all computed parametric values in all age groups, a fact supported by Siemionow et al. [24], who also perceived no statistical significance between men and women at all disk levels after a comparative study. On the contrary, Wang et al. [25] reported that young men are more susceptible to disk degeneration than young women, most likely due to increased mechanical stress and physical injury, whereas, between the ages of 50 and 60 years, female disks appear to degenerate at a notably quicker rate than male disks, most likely as a result of decreased estrogen. Our results and other contradictory findings would appear to prove that the relationship between gender and IDD is still a controversy [12, 24–27].

Previous research demonstrated that lower IVDs showed a statistically higher rate of degeneration when compared to upper levels [28]. The significant metrics observed in our study between upper disks and lower lumbar disks corroborated this assertion. Because of increased compressive loads at lower lumbar disks, a more robust elevation in matrix metalloproteinases (MMPs) of the extracellular matrix could trigger an increased rate of IDD [28]. Such an action would trigger a change in MK, MD, and FA values, which would provide ample evidence that IDD is more likely observed at lower lumbar disks clinically.

According to ROC, MK showed the highest diagnostic accuracy in differentiating Pfirrmann grade I from grade II disks and grade II from grade III disks, T2* coming last, preceded by MD and FA. This representation could be interpreted as DKI being a more sensitive technique than T2* mapping in early lumbar IDD. Also according to these results, as biomarkers of tissue microstructure and water molecules diffusion, MK and MD could sensitively detect IDD at an early stage. Reduced contents of PG and water are supposed to be the main changes at the earliest stages of degeneration, which is particularly notable in NP [28]. With disk degeneration, the increase in MK value potentially implied an increase in microstructure complexity by reason of the change of osmotic swelling and other factors; the decrease in MD value suggested a reduction in water, which indirectly indicated a loss in PG content. As a result, MK and MD derived from DKI served as robust biochemical markers of early IDD. Moreover, both DKI-related parameters and T2* showed better outcomes in NP than in AF when compared to the AUC, sensitivity, and specificity values in different segments. Therefore, MK, MD, FA, and T2* appeared to be sensitive to not only water and PG contents but also collagen integrity and more sensitive to water and PG contents. What is more, MK and MD might provide superior information on the biomechanical properties of early IDD, which would be helpful in prognoses and in improving therapy strategies.

This study still had some limitations. Firstly, due to anatomy, the pulsation of the abdominal aorta may interfere unavoidably with the AAF, which would incidentally affect the accuracy of measurement. Secondly, we did not compare the results with physical symptoms, though we plan to investigate the relationship between physical symptoms and MR quantitative measures in the future. Lastly, our study lacked histologic confirmation, with a detailed histologic evaluation scheduled in the future.

In conclusion, we demonstrated the feasibility of quantitatively assessing human IDD in vivo by using a DKI model. The results obtained with both the DKI and T2* mapping comparatively identified valuable biochemical parameters in the association between IDD and Pfirrmann grades at disk levels. Moreover, DKI was more sensitive to the quantitative detection of early lumbar IDD than T2* mapping.

Acknowledgements This study was supported by the grants from National Natural Science Foundation of China (No. 81871332) and Hubei Key Laboratory of Medical Information Analysis and Tumor Diagnosis & Treatment (No. PJS140011708).

Compliance with ethical standards

Conflict of interest All authors declare that they have no conflict of interest.

Ethical approval All procedures performed in studies involving human participants were in accordance with the ethical standards of the institutional and/or national research committee and with the 1964 Dec-

laration of Helsinki and its later amendments or comparable ethical standards.

References

1. Nilsson M, Lagerstrand K, Kasperska I, Brisby H, Hebelka H (2016) Axial loading during MRI influences T2-mapping values of lumbar discs: a feasibility study on patients with low back pain. Eur Spine J 25:2856–2863
2. Messner A, Stelzeneder D, Trattnig S et al (2017) Does T2 mapping of the posterior annulus fibrosus indicate the presence of lumbar intervertebral disc herniation? A 3.0 Tesla magnetic resonance study. Eur Spine J 26:877–883
3. Rajasekaran S, Naresh-Babu J, Murugan S (2007) Review of postcontrast MRI studies on diffusion of human lumbar discs. J Magn Reson Imaging 25:410–418
4. Newell N, Little JP, Christou A, Adams MA, Adam CJ, Masouros SD (2017) Biomechanics of the human intervertebral disc: a review of testing techniques and results. J Mech Behav Biomed Mater 69:420–434
5. Zhang XJ, Yang L, Gao F, Yuan ZG, Wang GB (2015) Comparison of T1ρ and T2* relaxation mapping in patients with different grades of disc degeneration at 3T MR. Med Sci Monit 21:1934–1941
6. Detiger SE, Holewijn RM, Hoogendoorn RJ, Royen BJ, Smit TH (2015) MRI T2* mapping correlates with biochemistry and histology in intervertebral disc degeneration in a large animal model. Eur Spine J 24:1935–1943
7. Kolf AK, Hesper T, Schleich C, Hosalkar H, Bittersohl B (2016) T2* mapping of ovine intervertebral discs: normative data for cervical and lumbar spine. J Orthop Res 34:717–724
8. Alkalay RN, Burstein D, Westin CF, Meier D, Hackney DB (2015) MR diffusion is sensitive to mechanical loading in human intervertebral disks ex vivo. J Magn Reson Imaging 41:654–664
9. Jensen JH, Helpern JA (2010) MRI quantification of non-Gaussian water diffusion by kurtosis analysis. NMR Biomed 23:698–710
10. Arab A, Wojna-Pelczar A, Khairnar A, Szabo N, Ruda-Kucerova J (2018) Principles of diffusion kurtosis imaging and its role in early diagnosis of neurodegenerative disorders. Brain Res Bull 139:91–98
11. Jensen JH, Helpern JA, Ramani A, Lu HZ, Kaczynski K (2005) Diffusional kurtosis imaging: the quantification of non-Gaussian water diffusion by means of magnetic resonance imaging. Magn Reson Med 53:1432–1440
12. Li L, Zhu WZ, Chen WW, Fang JC, Li J (2017) The study of the intervertebral disc microstructure in matured rats with diffusion kurtosis imaging. Magn Reson Imaging 42:101–106
13. Falk Delgado A, Nilsson M, Westen DV, Delgado AF (2018) Glioma grade discrimination with mr diffusion kurtosis imaging: a meta-analysis of diagnostic accuracy. Radiology 287:119–127
14. Das SK, Yang DJ, Wang JL, Zhang C, Yang HF (2017) Non-Gaussian diffusion imaging for malignant and benign pulmonary nodule differentiation: a preliminary study. Acta Radiol 58:19–26
15. Jiang JX, Tang ZH, Zhong YF, Su JY, Wu FY (2017) Diffusion kurtosis imaging for differentiating between the benign and malignant sinonasal lesions. J Magn Reson Imaging 45:1446–1454
16. Yin JZ, Sun HZ, Wang ZY, Ni HY, Sun PZ (2018) Diffusion kurtosis imaging of acute infarction: comparison with routine diffusion and follow-up MR imaging. Radiology 287:651–657
17. Xiao Z, Tang Z, Qiang J, Qian W, Tang W (2018) Differentiation of olfactory neuroblastomas from nasal squamous cell carcinomas using MR diffusion kurtosis imaging and dynamic contrast-enhanced MRI. J Magn Reson Imaging 47:354–361
18. Pfirrmann CW, Metzdorf A, Zanetti M, Hodler J, Boos N (2001) Magnetic resonance classification of lumbar intervertebral disc degeneration. Spine 26:1873–1878
19. Lazar M, Jensen JH, Xuan L, Helpern JH (2008) Estimation of the orientation distribution function from diffusional kurtosis imaging. Magn Reson Med 60:774–781
20. Lotz JC, Haughton V, Boden SD, An HS, Marinelli NL (2012) New treatment and imaging strategies in degeneration disease of the intervertebral disks. Radiology 264:6–19
21. Urban JP, Winlove CP (2007) Pathophysiology of the intervertebral disc and the challenges for MRI. J Magn Reson Imaging 25:419–432
22. Kim KW, Chung HN, Ha KY, Lee JS, Kim YY (2009) Senescence mechanisms of nucleus pulposus chondrocytes in human intervertebral discs. Spine J 9:658–666
23. Takatalo J, Karppinen J, Niinimäki J, Taimela S, Tervonen O (2012) Association of modic changes, Schmorl's nodes, spondylolytic defects, high-intensity zone lesions, disc herniations, and radial tears with low back symptom severity among young Finnish adults. Spine 37:1231–1239
24. Siemionow K, An H, Masuda K, Andersson GB, Cs-Szabo G (2011) The effects of age, sex, ethnicity, and spinal level on the rate of intervertebral disc degeneration: a review of 1712 intervertebral discs. Spine (Phila Pa 1976) 36:1333–1339
25. Wang YX, Griffith JF (2010) Effect of menopause on lumbar disc degeneration: potential etiology. Radiology 257:318–320
26. Gübitz R, Lange T, Gosheger G, Heindel W, Schulte TL (2018) Influence of age, BMI, gender and lumbar level on T1ρ magnetic resonance imaging of lumbar discs in healthy asymptomatic adults. Rofo 190:144–151
27. Oh CH, Yoon SH (2017) Whole spine disc degeneration survey according to the ages and sex using Pfirrmann disc degeneration grades. Korean J Spine 14:148–154
28. Zhang W, Ma XH, Wang Y, Zhao J, Li SL (2014) Assessment of apparent diffusion coefficient in lumbar intervertebral disc degeneration. Eur Spine J 23:1830–1836

Affiliations

Feifei Zeng[1] · Yunfei Zha[1] · Liang Li[1] · Dong Xing[1] · Wei Gong[1] · Lei Hu[1] · Yang Fan[2]

[1] Department of Radiology, Renmin Hospital of Wuhan University, 99, Zhangzhidong Road, Wuhan 430060, Hubei, China

[2] GE Healthcare China, Beijing, China